

Analysis of Actuation for a Spherical Robot

QingXuan Jia, HanXv Sun and DaLiang Liu

School of Automations

Beijing University of Posts and Telecommunications

Beijing, China

Dadi.liuwu@yahoo.com.cn

Abstract—In this paper, we present a spherical robot, which is steered and actuated through a counter-weight pendulum attached at a gimbal, a steer motor and a drive motor. The drive motor, linking gimbal and outer shell, generates the driving torque about the lateral rotation axis of the gimbal. The steer motor, located at the longitudinal axis of the gimbal, generates the leaning torque about longitudinal rotation axis. In this paper, we investigate its motion equations and non-holonomic constraints; develop the dynamic model, and present simulation study. The work is significant in understanding and developing this type of planning and controlling motions of nonholonomic systems.

Keywords—nonholonomic system, dynamics, spherical robot

I. INTRODUCTION

The lunar satellite, named Chang'e-1, was successfully launched in the autumn of 2007, marking the first step of China's ambitious three-stage moon mission and a new milestone in the country's space exploration history. One of the next missions is to launch lunar exploring rovers with the first successful soft landing on the surface in the near future.

Wheeled rovers are very complex and expensive, with limited ability to traverse rough terrain. Landing sites must be chosen that will ensure the safety of the rover and its ability to carry out a mission. Therefore, many scientifically interesting sites are inaccessible by current rover designs; the vast majority of our knowledge of the Moon is from data obtained by orbiting spacecraft. To gain a better understanding of the global picture of Moon from an up-close surface perspective, a new capability is needed that can transport scientific instruments across hundreds or even thousands of kilometers of varied Moon terrain.

One promising design configuration for a robot that could operate in such difficult terrain is to encapsulate the robot inside a spherical shell, and use this shell to make the robot move around in the environment. The spherical shape allows the robot to face all kinds of obstacles and operating surfaces, since a rolling ball naturally follows the path of least resistance. Several engineers at NASA Langley Research Center (LaRC) were discussing the Mars Pathfinder mission, which utilized a novel landing and deployment system of air bags, and joked that the air bag system allowed Pathfinder to travel a significant distance across the surface of Mars, much farther than the tiny, wheeled Sojourner rover ultimately would accomplish on its own. The Jet Propulsion Laboratory (JPL) concept is derived from the inflatable technology research program that developed



Figure 1. Photograph of the spherical robot

the Mars Pathfinder air bag system and is investigating inflatable rover designs[1]. However, a number of serious questions were posed: *What if the air bags were never deflated and Pathfinder were allowed to keep rolling? How could rolling be maintained? Could the wind be used to keep it rolling, like a tumbleweed plant?*

Fortunately, in recent years, to solve the motion of the spherical "bags", some working prototypes have been successfully constructed [2-10]. The spherical robot is a novel, omni-directional spherical mobile robot, originally developed in our laboratory [2]. Three prototypes have already been developed. Fig.1 shows the photograph of the third prototype. Essentially, the robot is a spherical shell, with an actuation mechanism fitted inside the shell. The actuation mechanism consists of two separate actuators: (1) a steer motor, which mainly controls the steering motion of the robot by tilting the counter-weight pendulum, and (2) a drive motor, which causes forward and/or backward acceleration by swinging the counter-weight pendulum indirectly through the gimbal. And the main axes of the two motors are perpendicular. Torques generated by the drive motor-reacting against the internal mechanism hanging as a counter-weight pendulum from the center of the gimbal's longitude axis- produce thrust for acceleration and braking. In fact, in the median coronal plane (Fig. 2b: X_B, Z_B coordinate system), the steer motor can be also produce thrust for the rolling motion plane along the longitude axis of the shell. But in this case, lacking the effective steering control, the motion and model of the system is more complex, and unstable, and not as the main object to study in this paper.

This configuration conveys significant advantages over multi-wheel, statically stable vehicles. These advantages include good dynamic stability, high maneuverability, low rolling resistance, ability to omni-directionally roll, and amphibious capability. Most important, the robot can resume stability even if a collision happened. So it is very suitable to be used in those unfriendly or harsh environments, such as outer planets and fields.

At the same time, spherical robot concept also brings a number of challenging problems in modeling and control. First, there are highly coupled dynamics among the shell, the gimbal and the counter-weight pendulum. This is similar to the case when a manipulator is mounted on a satellite [11]. Second, it is subject to a kind of non-holonomic system that can control more degrees of freedom using less drive inputs. The constraints arise when the robot rolls on the ground without slipping.

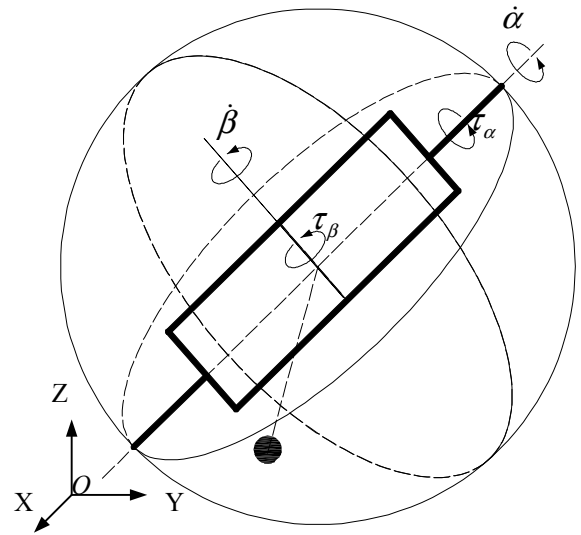
Thus far, the robot presented in this paper has been controlled only manually, using two joysticks to control the drive and steer motors through a radio link. A complete dynamic model is necessary to develop automatic control of the system. Because the motion among the shell, the gimbal and the counter-weight pendulum is highly coupled with each other, we need to consider the dynamics of the shell, the gimbal and counter-weight pendulum at the same time. In this paper, we derive the dynamic model using the constrained generalized Lagrangian formulation. We investigate the dynamic behavior and nonholonomic constraints of the system. Finally, we present simulate study at different initial conditions.

II. MATHEMATICAL MODEL

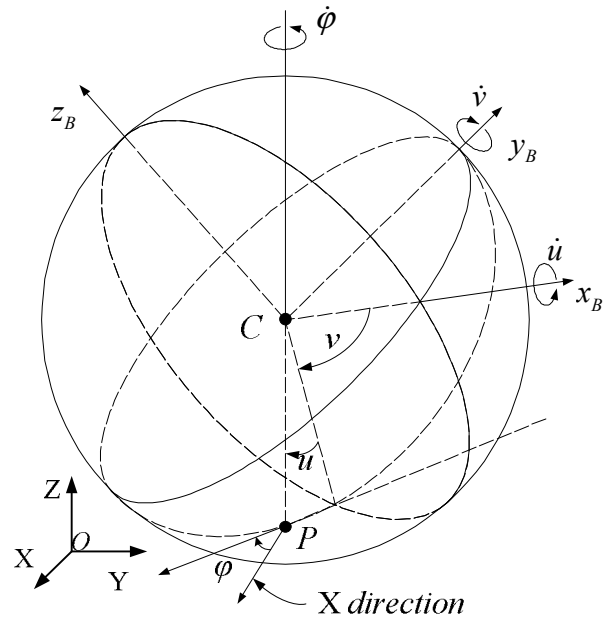
In derivation of the equations of motion of the robot, we assume that the shell is a rigid, homogeneous ball which rolls over a perfectly flat surface without slipping.

A. Coordinate frame

Let $\Sigma_o\{X, Y, Z\}$ and $\Sigma_B\{x_B, y_B, z_B\}$ be the inertial frame whose x - y plane is anchored to the flat surface and the body coordinate frame whose origin is located at the geometrical center of the rolling shell, respectively (Fig.2). Let (x_c, y_c, z_c) be the Cartesian coordinates of the center of mass of the shell (C) with respect to the inertial frame Σ_o , and assuming the geometrical center and the center of mass of the shell is the same point (C). Because of the swinging motion and the tilting motion of the counter-weight pendulum, the spherical robot has more degrees of freedom (**DOF**) than a typical rolling ball. Hence, we need to define two more frames: the coordinate frame of the internal gimbal $\Sigma_G\{X_G, Y_G, Z_G\}$ that is located at point (C) and whose x axis is always parallel to x_B (Fig.2b), and the counter-weight pendulum coordinate frame $\Sigma_P\{X_P, Y_P, Z_P\}$, which is located at the center of mass of the pendulum. Let (P) denote the point of contact on the plane (Fig. 2b).



(a) Configuration of the system



(b) Orientation of the shell

Figure 2. Robot model

B. Nonholonomic constraints

Rolling without slipping is a typical example of a non-holonomic system, since in most cases, some of the constrained equations for the system are non-integrable. Thus, the spherical robot is a similar type of the non-holonomic system. We define (i, j, k) and (l, m, n) to be the unit vectors of the coordinate system $\Sigma_o\{X, Y, Z\}$ and $\Sigma_B\{x_B, y_B, z_B\}$, respectively. Let $Sx := \sin(x)$ and $Cx := \cos(x)$. The transformation between the two coordinate frames given by

$$\begin{bmatrix} i \\ j \\ k \end{bmatrix} = R_B^O \begin{bmatrix} l \\ m \\ n \end{bmatrix} \quad (1)$$

Where $R_B^O \in SO(3)$ is the rotational matrix from Σ_O to Σ_B .

Let $\omega_s \in \mathbb{R}^3$ denote the angular velocity of the shell with respect to the inertia frame Σ_O . Then, we have

$$\omega_s = i\dot{l} + (\dot{\phi}Su + \dot{v})m + (\dot{\phi}Cu)n \quad (2)$$

The rolling constraint dictates that the instantaneous velocity of the bottom contact should be zero. The condition of absence of slipping thus becomes

$$\begin{aligned} v_p &= v_c + \omega_s \times r = 0 \\ r &= -Rk \end{aligned} \quad (3)$$

Where v_p, v_c are the velocity vectors of the point of contact and the center of mass of the shell, r is the vector directed from the center of mass (**C**) to the point of contact (**P**), and R is radius of the shell. Then, the kinematic constraints of the robot are

$$\dot{X}_c = R(\dot{u}S\phi + \dot{v}C\phi Cu) \quad (4)$$

$$\dot{Y}_c = R(\dot{u}C\phi - \dot{v}S\phi Cu) \quad (5)$$

$$\dot{Z}_c = 0 \rightarrow Z_c = R \quad (6)$$

Equations (4) and (5) are nonintegrable (i.e. non-holonomic), while equation (6) is integrable. Under the perfect rolling assumption, the spherical robot system is completely described by the kinematic constraints of contact between the shell and the plate. Note that the above kinematic model is not valid when $u = \pm\pi/2$.

In engineering, one often wants to consider the mechanical system not just from the point of view of analytical mechanics but also from the point of view of control systems. In analytical mechanics the equations of motion for a dynamical system are obtained with emphasis on describing the behavior of the mechanical system. In the control systems approach one seeks instead to identify exogenous input signals, obtain input/output formulations and prescribe desired system responses. To advance our understanding of the spherical robot system beyond what is afforded by kinematics, we will derive the dynamic equations.

C. Dynamics of the spherical robot

The analysis above indicates that the robot can be represented by seven generalized coordinates (e.g., $X_c, Y_c, u, v, \phi, \alpha, \beta$). We now derive the equations of motion by calculating the Lagrangian $L = T - P$ of the system, where **T** and **P** are the kinetic energy and potential energy of the system respectively. We divide the system into three parts: 1) shell, 2) gimbal, 3) counter-weight pendulum.

1) *shell*: The kinetic energy of the shell is given by

$$T_s = \frac{1}{2}m_s[\dot{X}_c^2 + \dot{Y}_c^2 + \dot{Z}_c^2] + \frac{1}{2}[I_{xxs}\omega_{sx}^2 + I_{yys}\omega_{sy}^2 + I_{zsz}\omega_{sz}^2]. \quad (7)$$

Assuming the shell is thinner, the principal moments of inertia of shell with respect to the center (**C**) are $I_{sx} = I_{sy} = I_{sz} = 2/5m_sR^2 = I_s$

The potential energy of the shell is constant $P_s = const.$

The Lagrangian of the shell is

$$L_s = \frac{1}{2}m_s[\dot{X}_c^2 + \dot{Y}_c^2] + \frac{1}{2}[I_{sx}\dot{u}^2 + I_{sy}(\dot{\phi}Su + \dot{v})^2 + I_{sz}(\dot{\phi}Cu)^2] - P_s \quad (8)$$

2) *Gimbal*:

Let T'_G denote the translational kinetic energy of the gimbal

$$T'_G = \frac{1}{2}m_G[\dot{X}_c^2 + \dot{Y}_c^2] \quad (9)$$

Let $\omega_G \in \mathbb{R}^3$ denote the angular velocity of the gimbal with respect to the inertia frame Σ_O . Then, we have

$$\omega_G = i\dot{l} + (\dot{\phi}Su + \dot{\alpha})m + (\dot{\phi}Cu)n \quad (10)$$

The rotational kinetic energy of the gimbal is now given by

$$T''_G = \frac{1}{2}[I_{Gx}\omega_{Gx}^2 + I_{Gy}\omega_{Gy}^2 + I_{Gz}\omega_{Gz}^2] \quad (11)$$

The principal moments of inertia of the gimbal with respect to the center (**C**)(Fig.2b) are assumed to be $I_{Gx} = I_{Gy} = I_{Gz} = I_G$

The potential energy of the gimbal is constant $P_G = const.$

The Lagrangian of the gimbal is

$$L_G = T'_G + T''_G - P_G. \quad (12)$$

3) *Counter-weight pendulum*:

Let (x_p, y_p, z_p) be the center of mass of the counter-weight pendulum with respect to Σ_O . The transformation from the center of mass of the shell to the point (**P**) can be described

$$\begin{bmatrix} x_p \\ y_p \\ z_p \end{bmatrix} = \begin{bmatrix} X_c \\ Y_c \\ Z_c \end{bmatrix} + IR_B^O R_p^B \begin{bmatrix} 0 \\ 0 \\ -1 \end{bmatrix}. \quad (13)$$

Where $R_p^B \in SO(3)$ is the transformation from Σ_p to Σ_B

Let T'_p denote the translational kinetic energy of the pendulum

$$T_p^i = \frac{1}{2} m_p [\dot{x}_p^2 + \dot{y}_p^2 + \dot{z}_p^2] \quad (14)$$

Differentiating (13) and substituting it in (14), we obtain T_p^i .

The potential energy of the counter-weight pendulum is

$$P_p = m_p g (R - l C \alpha C \beta) \quad (15)$$

Thus, the Lagrangian of the counter-weight pendulum can be written as

$$L_G = T_G^i - P_p. \quad (16)$$

Using the previous analysis, it can be shown that the Lagrangian of the overall system is

$$L = L_S + L_G + L_p. \quad (17)$$

Substituting (8), (12), and (16) into (17), L can be determined. It is noted that there are only two control torques available: the drive torque (τ_α) and the tilt torque (τ_β). Using the constrained Lagrangian method [13], the dynamic equation of the entire system is given by

$$M(q)\ddot{q} + N(q, \dot{q}) = A^T \lambda + B\tau. \quad (18)$$

Where $M(q) \in \mathbb{R}^{7 \times 7}$ and $N(q, \dot{q}) \in \mathbb{R}^{7 \times 1}$ are the inertia matrix and nonlinear term, respectively.

$$A(q) = \begin{bmatrix} 1 & 0 & -RS\varphi & -RC\varphi Cu & 0 & 0 & 0 \\ 0 & 1 & RC\varphi & -RS\varphi Cu & 0 & 0 & 0 \end{bmatrix} \quad (19)$$

$$q = \begin{bmatrix} X_C \\ Y_C \\ u \\ v \\ \varphi \\ \alpha \\ \beta \end{bmatrix}, \lambda = \begin{bmatrix} \lambda_1 \\ \lambda_2 \end{bmatrix}, B = \begin{bmatrix} 0 & 0 \\ 0 & 0 \\ 0 & 0 \\ 0 & 0 \\ 0 & 0 \\ 1 & 0 \\ 0 & 1 \end{bmatrix}, \tau = \begin{bmatrix} \tau_\alpha \\ \tau_\beta \end{bmatrix}.$$

The non-holonomic constraints can be written as

$$A(q)\dot{q} = \mathbf{0}_{2 \times 1}. \quad (20)$$

To obtain a minimum set of differential equations, we need to eliminate the Lagrange multipliers. We first partition the matrix $A(q)$ into A_1 and A_2 , where $A = [A_1 : A_2]$.

$$A_1 = \begin{bmatrix} 1 & 0 \\ 0 & 1 \end{bmatrix}, \quad A_2 = \begin{bmatrix} -RS\varphi & -RC\varphi Cu & 0 & 0 & 0 \\ RC\varphi & -RS\varphi Cu & 0 & 0 & 0 \end{bmatrix} \quad (21)$$

Let

$$C(q) = \begin{bmatrix} -A_1^{-1} A_2 \\ I_{5 \times 5} \end{bmatrix}. \quad (22)$$

Next consider the following relationship:

$$\dot{q} = C(q)\dot{q}_2 \quad (23)$$

Where $\dot{q}_1 = [\dot{X}_C \ \dot{Y}_C]^T$ and $\dot{q}_2 = [\dot{u} \ \dot{v} \ \dot{\varphi} \ \dot{\alpha} \ \dot{\beta}]^T$. Differentiating (23) yields

$$\ddot{q} = C(q)\ddot{q}_2 + \dot{C}(q)\dot{q}_2. \quad (24)$$

Substituting (20) into (18) and multiplying both sides by $C^T(q)$ gives

$$C^T(q)M(q)C(q)\ddot{q}_2 = C^T(q)[B\tau - N(q, C(q)\dot{q}_2) - M(q)\dot{C}(q)\dot{q}_2]. \quad (25)$$

Where $C^T(q)M(q)C(q)$ is a 5x5 symmetric positive definite matrix function. $C^T(q)M(q)C(q)$ can be treated as a new inertia matrix with respect to the new set of generalized coordinates ($u, v, \varphi, \alpha, \beta$). By numerical integration, we can obtain q_2 from \ddot{q}_2 in (25), and then obtain (X_C, Y_C) by substituting q_2 and \dot{q}_2 in (23).

D. Model Simplification

The expressions of the system (25) are particularly lengthy, not adapted to develop this type of planning and controlling motions, and need be simplified.

Noting that the relative angular displacements (i.e. the swinging and tilting angle) α and β are not important from the perspective of our control objects, they should be omitted in the simplified model. Furthermore, in the steady motion, the swinging and tilting angle of the internal mechanism (i.e. gimbal and counter-weight pendulum) is sufficiently small [14]. This brings up the question of whether or not α and β can be neglected. We consider the dynamics of the gimbal and the pendulum describing the swinging motion. Let the drive torque τ_α applied on the gimbal and the pendulum by the drive motor. In the steady motion, the rolling speed of the shell is around a certain nominal rolling speed with a small angular acceleration. The dynamics of the gimbal and the pendulum can be described as

$$-m_p g l S \alpha C \beta = \tau_\alpha = (I_{SX} + I_{GX})\ddot{v} \quad (26)$$

Then

$$\sin \alpha = -\frac{(I_{SX} + I_{GX})\ddot{v}}{m_p g l C \beta} \quad (27)$$

In the steady motion, the angular acceleration \ddot{v} is sufficiently small and assuming that the mass of the pendulum

is much greater than the gimbal and the shell, even though the tilting angle β is closer to $\pm\pi/2$, we have $\sin\alpha = \alpha \approx 0$. And similarly we have $\sin\beta = \beta \approx 0$.

Using the previous derivation and assumptions, the equations of the entire system are written

$$\bar{M}(\bar{q})\ddot{\bar{q}} = \bar{F}(\bar{q}, \dot{\bar{q}}) + \bar{B}\tau. \quad (28)$$

where $\bar{q} = [u \ v \ \varphi \ \alpha \ \beta]^T$

$$\bar{M} = \begin{bmatrix} \bar{M}_{11} & 0 & 0 & 0 & 0 \\ 0 & \bar{M}_{22} & I_S(Su) & 0 & 0 \\ 0 & I_S(Su) & \bar{M}_{33} & \bar{M}_{34} & 0 \\ 0 & 0 & \bar{M}_{34} & \bar{M}_{44} & 0 \\ 0 & 0 & 0 & 0 & I_p \end{bmatrix}$$

$$\bar{F} = [\bar{F}_1 \ \bar{F}_2 \ \bar{F}_3 \ \bar{F}_4 \ \bar{F}_5]^T \quad \bar{B} = B$$

$$\bar{M}_{11} = mR^2 + I_S + I_G, \bar{M}_{22} = mR^2(Cu)^2 + I_S, \bar{M}_{33} = I_G + I_S + I_G$$

$$\bar{M}_{44} = I_p + I_G, \bar{M}_{34} = (I_p + I_G)Su$$

$$\bar{F}_1 = (mR^2 + I_S)Cu\dot{v}\dot{\varphi} + (I_p + I_G)(Cu)^2\dot{\varphi}\dot{\alpha} - m_p g l S \beta C \alpha$$

$$\bar{F}_2 = -(mR^2 + I_S)Cu\dot{u}\dot{\varphi} - \frac{1}{2}mR^2 S(2u)\dot{u}\dot{v} - m_p g l C \beta S \alpha$$

$$\bar{F}_3 = -I_S C u \dot{u} \dot{\varphi} - (I_p + I_G) C u \dot{u} \dot{\alpha}$$

$$\bar{F}_4 = -(I_p + I_G) C u \dot{\varphi} \dot{u} - 2m_p g l C \beta S \alpha$$

$$\bar{F}_5 = -2m_p g l S \beta C \alpha$$

$$m = m_s + m_p + m_G$$

where $\bar{M}(\bar{q}) \in \mathbb{R}^{5 \times 5}$ and $\bar{F}(\bar{q}, \dot{\bar{q}}) \in \mathbb{R}^{5 \times 1}$ are the inertia matrix and nonlinear term of the system, respectively.

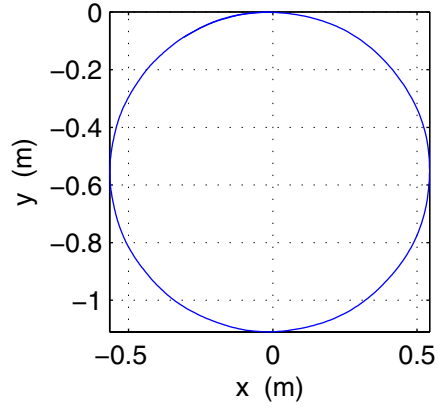
Equation (28) shows the reduced dynamic model of the robot, unlike typical underactuated systems, the lean angle u is not coupled with the spinning angle v and the steering angle φ at the acceleration level, they are coupling at the velocity level through the cross terms \dot{v} and $\dot{\varphi}$.

III. SIMULATION STUDY

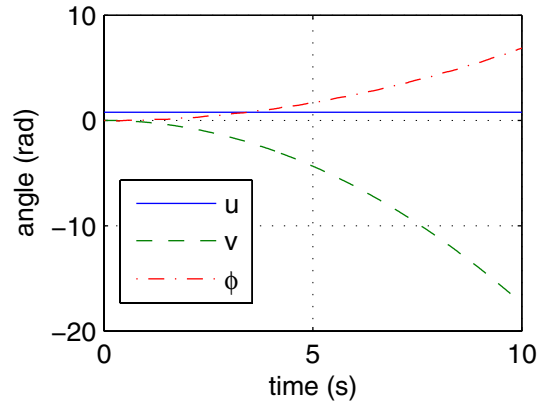
We illustrate the results of the paper with a simulation example, the system parameters are given by

$$\begin{cases} m = 25 \text{ kg} & m_p = 6 \text{ kg} \\ I_S = 0.3 \text{ kg} \cdot \text{m}^2 \\ I_G = 0.1 \text{ kg} \cdot \text{m}^2 \\ I_p = 0.1 \text{ kg} \cdot \text{m}^2 \\ R = 0.3 \text{ m} & l = 0.15 \text{ m} \end{cases} \quad (29)$$

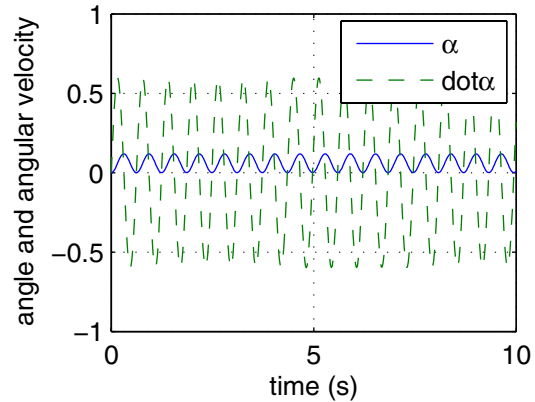
Fig.3 shows the simulation results under the initial conditions in which the rolling rate of the shell was set to be zero as followed



(a) x-y plot



(b) Time evolution of posture of the shell



(c) Time evolution of the pendulum

Figure 3. Simulation results under the conditions in (30)

$$\begin{cases} \dot{u} = \dot{u}_0 = \dot{\varphi}_0 = \dot{v}_0 = 0 \text{ rad/s} \\ u_0 = \pi/4 \text{ rad} & v_0 = \varphi_0 = 0 \text{ rad} \\ \tau_\alpha = 1 \text{ N} \cdot \text{m} & \tau_\beta = 0 \text{ N} \cdot \text{m} \end{cases} \quad (30)$$

And the simulation takes about 10 sec. From Fig.3a, the robot trajectory is nearly a circular path, and similar to a rolling gyroscope. As for a rolling gyroscope, if the inclination is not $\pm\pi/2$, it processes the direction it leans, thus it normally

travels in a circular trajectory. At the same time, we noted that the motion of the counter-weight pendulum is oscillate in nature, and the angular velocity varies between zero and a positive maximum value (Fig.3c).

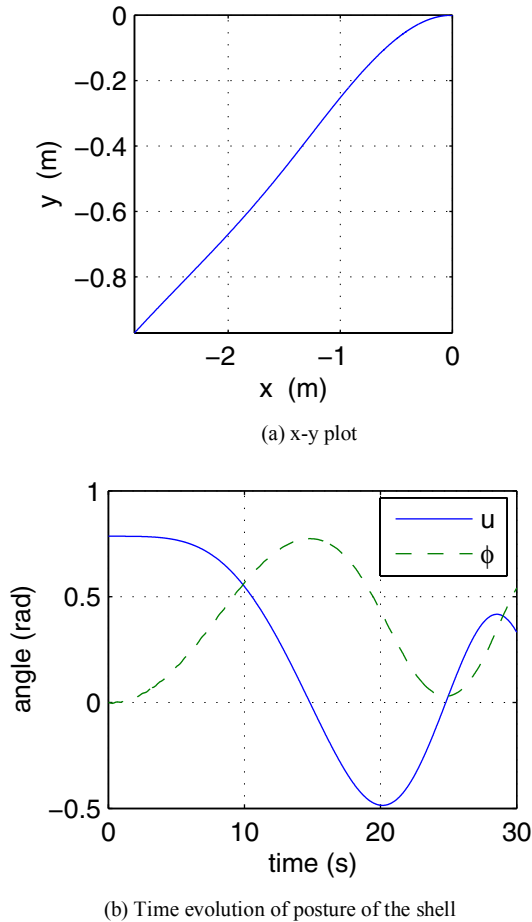


Figure 4. Simulation results under the conditions in (31)

Fig.4 shows the second simulation results. The simulation conditions are

$$\begin{cases} \dot{u}_0 = \dot{\phi}_0 = \dot{v}_0 = 0 \text{ rad} / \text{s} \\ u_0 = \pi / 4 \text{ rad} & v_0 = \phi_0 = 0 \text{ rad} \\ \tau_\alpha = 0.1 \text{ N} \cdot \text{m} & \tau_\beta = 0 \text{ N} \cdot \text{m} \end{cases} \quad (31)$$

and the simulation takes about 30 sec. In this case, owing the coupled effect between leaning motion and spinning motion at the velocity level, if the shell rolls rapidly in the median sagittal plane, the lean angle u will vary rapidly and damply oscillate. This characteristic of the motion imposes the difficult to stabilize and control the spherical robot.

IV. CONCLUSION

In this paper, we first studied the velocity constraints for the robot. Then we developed the dynamic model using the constrained Lagrangian method. Based on the simulation, we found that the property of the robot is similar to a rolling gyroscope if its shell does not rotate in the median coronal

plane. According to the conclusion, the robot can be steered to where it intends to go. The simulation study based on the dynamic model of the robot is significant for us to understand the dynamic behavior of the system, and guide us in the automatic control of the robot.

ACKNOWLEDGMENT

The authors wish to acknowledge the support provided by National Natural Science Foundation of China (50775013), and China National High-Tech Research and Development (863) Plan (2006AA04Z243).

REFERENCES

- [1] (2007,Oct.) Tumbleweed Inflatable Rover. [Online]. Available: <http://www2.jpl.nasa.gov/adv/tech/rovers/tumbleweed.htm>.
- [2] H.X.Sun, A.P. Xiao, Q.X. Jia and L.Q. Wang, "Omnidirectional kinematics analysis on bi-driver spherical robot", Journal of Beijing University of Aeronautics and Astronautics, vol. 31, pp. 735-739. July. 2005, Language: Chinese.
- [3] T.Kumar, Das, "Feedback stabilization of the rolling sphere: An Intractable Nonholonomic System," 300 North Zeeb Road, USA: ProQuest Information and Learning Company, 2002.
- [4] M. Seeman, M. Broxvall, A. Saffiotti and P. Wide, "An Autonomous Spherical Robot for Security Tasks", Proc. IEEE Int. Conf. on Computational Intelligence for Homeland Security and Personal Safety, Oct. 2006, pp. 51-55.
- [5] Q. Zhan, T. Zhou, M. Chen and S.-L. Cai, "Dynamic Trajectory Planning of a Spherical Mobile Robot", Proc. IEEE Int. Conf. on Robotics, Automation and Mechatronics, Dec.2006, pp.1-6.
- [6] M. Yue, Z.Q. Deng, X.Y. Yu, and W.Z. Yu, "Introducing HIT Spherical Robot: Dynamic Modeling and Analysis Based on Decoupled Subsystem", Proc. IEEE Int. Conf. Robotics and Biomimetics, Dec. 2006, pp.181 - 186.
- [7] S. Bhattacharya and S. K. Agrawal, "Spherical Rolling Robot: A Design and Motion Planning Studies", IEEE Trans. Robotics and Automation, vol. 16, 2000, pp.835-839.
- [8] A. Bicchi, A. Balluchi, D. Prattichizzo and A. Grelli, "Introducing the Sphericle: An Experimental Testbed for Research and Teaching in Nonholonomy", Proc. IEEE Int. Conf. on Robotics and Automation, Albuquerque, New Mexico, 1997, pp.2620-2625.
- [9] J. Alves and J. Dias, "Design and Control of a Spherical Mobile Robot", Proc. of the IMechE Part I: Journal of System and Control Engineering, vol. 217, 2003, pp.457-467.
- [10] A. H. Javadi A. and P. Mojabi, "Introducing glory: A Novel Strategy for an Omnidirectional Spherical Rolling Robot", Trans. of the ASME. Journal of Dynamic Systems, Measurement and Control, vol. 126, 2004, pp.678-683.
- [11] Y. Xu and H. Y. Shum, "Dynamic control and coupling of a free-flying space robot system," J. Robotic Syst., vol. 11, 1994, pp.573-589.
- [12] Z.Li and J.Canny. "Motion of two rigid bodies with rolling constraint," IEEE Trans. on Robotics and Automation, 6(1), 1990.
- [13] J. H. Ginsberg, Advanced Engineering Dynamics. Cambridge, U.K.. Cambridge Univ. Press, 1995.
- [14] Y.-S. Xu and S. K.-W. Au, "Stabilization and Path Following of a Single Wheel Robot", IEEE Trans. On Mechatronics., vol. 9, pp. 407-419, June. 2004.